2015 IEEE Wireless Communications and Networking Conference (WCNC) - Workshops - 2nd International Workshop on Device-to-Device and Public Safety Communications

UAV Assisted Heterogeneous Networks for Public Safety Communications

Arvind Merwaday and İsmail Güvenç
Dept. of Electrical and Computer Engineering, Florida International University,
10555 W Flagler St, EC 3900, Miami, FL 33174
Email: {amerw001, iguvenc}@fiu.edu

***Abstract*—Communications play an important role during public safety operations. Since the current communication technologies heavily rely on the backbone network, the failure of base stations (BSs) due to natural disasters or malevolent attacks causes communication difficulties for public safety and emergency communications. Recently, the use of unmanned aerial vehicles (UAVs) such as quadcopters and unmanned gliders have gained attention in public safety communications. They can be used as unmanned aerial base stations (UABSs), which can be deployed rapidly as a part of the heterogeneous network architecture. However, due to their mobile characteristics, interference management in the network becomes very challenging. In this paper, we explore the use of UABSs for public safety communications during natural disasters, where part of the communication infrastructure becomes damaged and dysfunctional (e.g., as in the aftermath of the 2011 earthquake and tsunami in Japan). Through simulations, we analyze the throughput gains that can be obtained by exploiting the mobility feature of the UAVs. Our simulation results show that when there is loss of network infrastructure, the deployment of UABSs at optimized locations can improve the *throughput coverage* and the 5th percentile spectral efficiency of the network. Furthermore, the improvement is observed to be more significant with higher path-loss exponents.**

***Index Terms*—5G, drone, interference coordination, LTE, public safety communications (PSC), quadcopter, unmanned aerial base stations, UAVs.**

I. Introduction

Public safety communications (PSCs) carry critical importance to save lives, property, and national infrastructure in case of incidents such as fires, terrorist attacks, or natural disasters. Up until recently, PSC has been handled through narrowband communication technologies such as the land mobile radio (LMR), which can deliver reliable voice communications, but do not support broadband data [1], and are also often limited in terms of coverage and interoperability [2]. The National Broadband Plan by the FCC states that a cutting-edge PSC shall make use of *broadband technologies* "to allow first responders anywhere in the nation to send and receive critical voice, video and data to save lives, reduce injuries and prevent acts of crime and terror", while acknowledging that *"the U.S. has not yet realized the potential of broadband to enhance public safety"* [3].

Broadband wireless technologies such as the 4G Long Term Evolution (LTE), and its foreseen 5G successor have a strong potential for revolutionizing communications during public safety situations. Driven by the need to meet the exponential increase in the demand for the wireless spectrum, research and standardization activities for 5G wireless networks are already underway – with an ambitious goal of 1000× capacity enhancement, 10× cell-edge user rate enhancement, and a 10× (to 1 ms) roundtrip latency reduction over 4G systems [4]. Exploiting such powerful features of 5G systems will be essential for transforming the PSC infrastructures from a capacity-limited platform into a high-speed communication infrastructure [5]. Indeed, the 3GPP standardization group has recently started working on developing public safety capabilities in LTE-Advanced to support the specific requirements of PSC [6]. Studies to develop the first nationwide, high-speed PSC network in the U.S., FirstNet [7], have also begun.

Another important opportunity for revolutionizing the PSC capabilities is to introduce UAVs, such as balloons, quadcopters, or gliders, for delivering pervasive broadband connectivity [8]. Enabled by recent technological advances, miniaturization, and open-source hardware/software initiatives, UAVs have found several key applications recently [9]-[12]. Amazon, for example, claims that seeing its *Prime Air* order delivery UAVs in the sky is expected to be as conventional as seing mail trucks on the road within the next few years [11]. Google and Facebook have been investigating the use of a network of high-altitude balloons [13] and drones [14] over specific population centers for providing broadband connectivity. Such solar-powered drones are capable of flying several years without refueling. A relatively less explored application of UAVs is to deliver broadband data rates in emergency and public safety situations through low-altitude platforms [15]. UAVs are uniquely suited for such PSC scenarios due to their mobility and

This research was supported in part by the U.S. National Science Foundation under the grant CNS-1406968.

978-1-4799-8760-3/15/$31.00 ©2015 IEEE

self organization capabilities, which are invaluable for quickly delivering broadband connectivity at times and locations where most needed, through an agile, low-cost, and ubiquitous communication infrastructure.

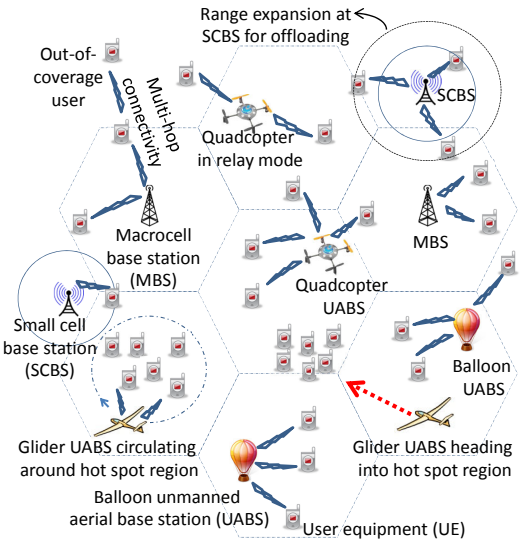

Fig. 1. Large scale PSC scenario. The MBSs, SCBSs, and UABSs constitute a heterogeneous network (HetNet) infrastructure, where the UABSs can dynamically change their positions for optimized coverage and seamless broadband connectivity.

II. Public Safety Communications Scenarios

This paper aims to explore a new generation of broadband PSC systems that include a synergistic use of 5G broadband and unmanned aerial vehicles (UAVs) for addressing the intricate interference management challenges in emerging PSC scenarios. In particular, the paper introduces a broadband and UAV-assisted heterogeneous network (BAHN) approach that will constitute the pillar of the next generation of PSC systems. To provide a context for the proposed BAHN system, two representative PSC scenarios are discussed next.

1) Scenario-1: Large-scale BAHN PSC scenario: The first typical public safety scenario, illustrated in Fig. 1, involves providing capable PSCs in diaster-affected environments following the aftermath of an earthquake, tsunami, or hurricane. In such environments, there is a vital need to maintain broadband, high-speed communication between first responders and victims, whose basic communication mediums may be jeopardized by damaged networking infrastructure as in the 2011 Earthquake in Japan [16]. In the representative scenario shown in Fig. 1, only two of the seven macrocell base stations (MBSs) with large coverage areas remain operational after a disaster. The figure also illustrates a number of small cell base stations (SCBSs), which can be critical to maintain connectivity in PSC scenarios. Range expansion techniques [17] are commonly used with the SCBSs to extend coverage and fairly distribute users among different cells. To sustain ubiquitous broadband connectivity, Fig. 1 shows how different types of UAVs are serving as unmanned aerial base stations (UABSs). In hot-spot regions with denser user equipment (UE) population, quadcopters can hover at a fixed location, while gliders have to follow a circular trajectory. Relaying and multi-hop communication methods can also be used for extending the coverage through the incident scene, either through UAVs or other UEs.

2) Scenario-2: Small-scale BAHN PSC scenario: A second, typical PSC scenario involves a smaller-scale BAHN environment as in Fig. 2, representative of scenarios such as a building on fire or a barricaded suspect. The incident scene is served by a number of SCBSs, which are embedded into police cars, fire trucks, and UAVs. These SCBSs provide broadband connectivity to first responders and victims in a timely manner, typically for deep situational awareness purposes through real-time wireless video streaming. Some example use cases of broadband connectivity include transmission of 3D blueprints of a burning building to the hand-held devices of first responders, live streaming of high definition video of the incident scene from the cap-mounted cameras (or Google-glass like gadgets) of the first responders to a command center, and transmission of multichannel vital signs of a hurt disaster victim to an external medical post to facilitate the diagnosis in collaboration with the on-site emergency medical staff and a remote specialist [5]. By exploiting UAV mobility, broadband connectivity can be delivered into desired regions, including congested areas and indoor environments.

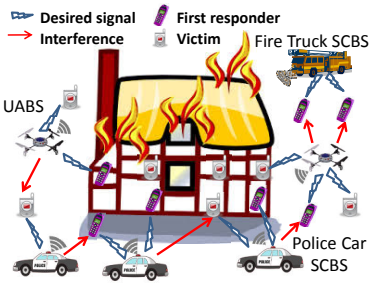

Fig. 2. Building fire scenario.

A major challenge in BAHNs is to address the severe and highly dynamic interference challenges during/after the disaster scenarios as shown in Fig. 1 and Fig. 2. When compared with conventional heterogeneous network (HetNet) interference management techniques, scenarios such as in Fig. 1 and Fig. 2 are particularly unique and challenging due to 1) potentially damaged BS infrastructure, yielding outage problems; 2) mobility of SCBSs in UAVs, police cars, and fire trucks, resulting in dynamic interference patterns and uncoordinated final locations of SCBSs; 3) dynamically changing locations of UEs following a disaster, potentially clustered into some hot-spot areas; 4) HetNet traffic with bursty data

transmission (e.g., post-earthquake) which may temporarily overload the network infrastructure; and 5) the need to maintain high QoS for public safety personnel in mission-critical scenarios.

In this paper, we focus on the large scale PSC scenario which is illustrated in Fig. 1. We assume the MBS locations are randomly distributed according to Poisson point process (PPP), and perform Monte Carlo simulations to evaluate capacity and *throughput coverage* of the network. We randomly remove some base station (BS) nodes to imitate a natural disaster, and then study the impact of infrastructure damage on the capacity and coverage. We also investigate the potential benefits of UAVs in the post disaster scenario by studying the capacity and coverage improvements achieved through the deployment of UAVs. Furthermore, we optimize the locations of the UAVs to maximize the 5th percentile capacity of the network.

III. System Model

We consider a cellular network with MBS and UE locations modeled as two-dimensional homogeneous PPPs of intensities λ and λ_{u}, respectively. PPP-based models may not be viable for capturing real MBS locations, due to some points of the process being very close to each other. However, the PPP-based models provide reasonably close performance results when compared with the real BS deployments [17]. We assume all the MBSs transmit at power P_{tx}, and every UE connects to its nearest MBS. For an arbitrary UE n at a distance r_{nm} from its serving MBS m, the average received signal power is given by

$$S(r_{nm}) = \frac{P_{\mathrm{tx}} K}{r_{nm}^{\delta}}, \tag{1}$$

where δ is the path-loss exponent (PLE), and K is the factor that accounts for the geometrical parameters such as transmitter and receiver antenna heights, etc. We consider an interference limited network in which the thermal noise power at a receiver is assumed to be negligible when compared to the interference power. Then, the SIR at UE n can be expressed as,

$$\Gamma_n = \frac{S(r_{nm})}{\sum_{i \in \mathcal{M}, i \neq m} S(r_{ni})}, \tag{2}$$

where $\mathcal{M}$ is the set of all MBSs, and r_{ni} is the distance of nth UE to the ith MBS. The denominator in (2) represents the total interference power at UE from all the MBSs except the serving MBS m. Using Shannon capacity formula, and considering round-robin scheduling for simplicity, the spectral efficiency (SE) of a macrocell UE (MUE) can be expressed as,

$$C_n = \frac{\log_2(1+\Gamma_n)}{N}, \tag{3}$$

where N is the number of MUEs in the macrocell.

A. Throughput Coverage

Since achieving broadband rates is considered as a major goal, a UE is considered to be in *throughput coverage* if its average throughput per unit bandwidth is higher than a threshold T_{C}, i.e., $C > T_{\mathrm{C}}$. Here, we assume full buffer traffic in all the downlinks. A sample network layout with MBS intensity $\lambda = 4$ per km^2 is illustrated in Fig. 3 for a 3×3 km^2 region.

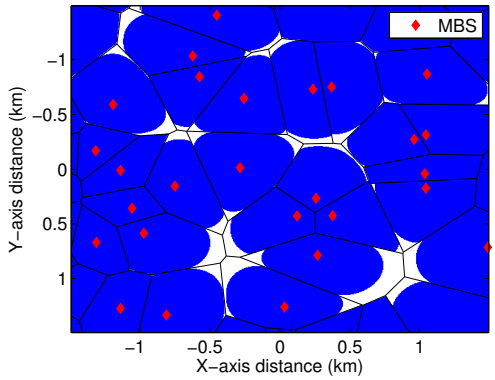

Fig. 3. Illustration of a network layout and throughput coverage. Parameter settings: $\lambda = 4$ per km^2, $\lambda_{\mathrm{u}} = 400$ per km^2, P_{tx} (in dBm) $=$ 46 dBm, and $T_{\mathrm{C}} = 3.5 \times 10^{-3}$ bps/Hz.

In Fig. 3, the black lines indicate the cell boundaries, while the blue colored areas correspond to the throughput coverage areas in which the UEs' throughput are greater than the threshold $T_{\mathrm{C}} = 3.5 \times 10^{-3}$ bps/Hz, assuming a UE intensity of $\lambda_{\mathrm{u}} = 400$ per km^2. The white colored regions, on the other hand, are areas where the user throughput is lower than the threshold T_{C}, which is negligible in Fig. 3.

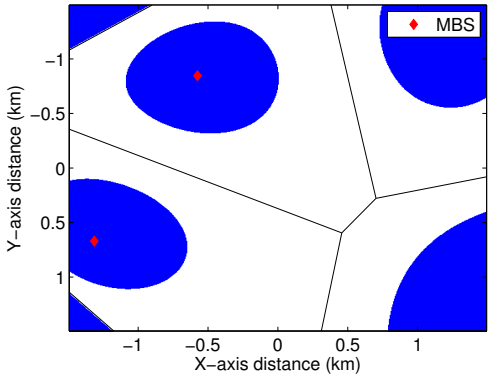

Fig. 4. Illustration of throughput coverage after an earthquake.

To illustrate the impact of infrastructure loss on coverage and throughput, an example scenario of the cellular network after an earthquake is shown in Fig. 4, where 90% of the MBSs are randomly destroyed during a disaster, and the same throughput threshold T_{C} as in Fig. 3 is used to calculate outage regions. In this second scenario, outage region grows significantly, due to 1) overloading of MBSs with many UEs, and 2) poor link qualities of UEs far away from the MBSs.

In a PSC scenario, first responders and victim users located within a white region in Fig. 4 will observe very low throughput, or even a complete outage and loss of connectivity. Naturally, for higher throughput thresholds, the outage region will grow even larger.

IV. Coverage Improvement Using UABSs

In the scenario of loss in network infrastructure as in Fig. 4, UABSs can be deployed rapidly to form small-cells and consequently improve the network coverage. Unlike MBSs, the UABSs' positions can be dynamically adjusted and therefore their physical locations can be optimized in order to get the best network performance for a given scenario.

With the deployment of UABSs, a HetNet is formed with two tiers of BSs: MBSs and UABSs. We assume that both the MBSs and the UABSs share a common transmission bandwidth. For simplicity, we assume that the wireless backhaul links of the UABSs have very large capacity, and they use a different frequency band than the access links. For an arbitrary UE n, let the nearest MBS m at a distance r_{nm} be its MBS of interest (MOI) and the nearest UABS u at a distance r_{nu} be its UABS of interest (UOI). Then, the average received signal power from the MOI and the UOI are respectively given by

$$S(r_{nm}) = \frac{P_{\text{tx}} K}{r_{nm}^{\delta}}, \quad S'(r_{nu}) = \frac{P'_{\text{tx}} K'}{r_{nu}^{\delta}}, \tag{4}$$

where P'_{tx} is the transmit power of UABSs, and K' is the factor that accounts for the geometrical parameters such as the transmitter and receiver antenna heights. Then, an arbitrary UE experiences the SIRs,

$$\Gamma_n = \frac{S(r_{nm})}{\sum_{i\in\mathcal{M}, i\neq m} S(r_{ni}) + \sum_{j\in\mathcal{U}} S'(r_{nj})}, \tag{5}$$

$$\Gamma'_n = \frac{S'(r_{nu})}{\sum_{i\in\mathcal{M}} S(r_{ni}) + \sum_{j\in\mathcal{U}, j\neq u} S'(r_{nj})}, \tag{6}$$

from the MOI and the UOI, respectively. Here, $\mathcal{U}$ is the set of all UABSs, and r_{nj} is the distance of nth UE to the jth UABS. The denominators of (5) and (6) represent the total interference power at the UE. We assume that the UABSs employ range expansion bias (REB) during the UE association process in order to associate with more number of UEs. Each UE performs cell selection by using Γ_n, Γ'_n and the REB τ as follows:

$$\text{If } \Gamma_n > \tau\Gamma'_n \rightarrow \text{select MOI}, \tag{7}$$

$$\text{If } \Gamma_n \leq \tau\Gamma'_n \rightarrow \text{select UOI}. \tag{8}$$

Finally, the SEs of MUE and UABS-cell UE (UUE) can be respectively expressed as,

$$C_n = \frac{\log_2(1+\Gamma_n)}{N}, \quad C'_n = \frac{\log_2(1+\Gamma'_n)}{N'}, \tag{9}$$

where N' is the number of UUEs in the UABS-cell.

TABLE I
System Parameters

Parameter	Description	Value
$\lambda, \lambda_{\text{u}}$	MBS and UE intensities	$4, 100$
$P_{\text{tx}}, P'_{\text{tx}}$ (in dBm)	MBS and UABS transmit powers	46 dBm, 30 dBm
K, K' (in dB)	Factors accounting for the geometrical parameters of antennas	-11 dB, -11 dB
δ	Path-loss exponent	4
τ	Range expansion bias	0 dB
d_{h}	Altitude of UABSs	400 feet
T_{C}	Throughput coverage threshold	2.55×10^{-3} bps/Hz
A_{sim}	Simulation area	10×10 km^2

Fig. 5 shows an optimized placement (through brute force search) of four UABSs, in a way to maximize the 5th percentile throughput over the whole network. Each UABS is assumed to know the locations of other UABSs and BSs. The UABSs are observed to be clustered around the cell edges in order to take over the low-SIR UEs in an effort to maximize 5th percentile rate. In the considered architecture, it is assumed that UABSs can communicate through a backhaul link to a nearby BS node [18], [19].

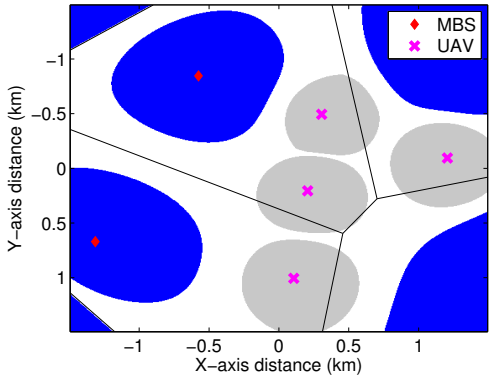

Fig. 5. Illustration of throughput coverage with UABSs after an earthquake.

V. Simulation Results

The ability of UABSs to move to any location and height on an incident area provides a powerful mechanism to maintain high throughput coverage throughout the network. To illustrate potential gains that can be obtained, we investigate how an optimized deployment of UABSs can improve the network throughput for the scenario of Fig. 5. Unless otherwise specified, the system parameters for the simulations were set to the values as shown in Table I, and the locations of all UABSs were optimized through brute force search to maximize 5th percentile SE of the network. We chose brute force search for simplicity; however, other optimization techniques can also be used for efficient implementation. The simulation area was divided into a grid, with horizontal and vertical distances of 0.5 km between the vertices. The 5th percentile SE was evaluated by placing the

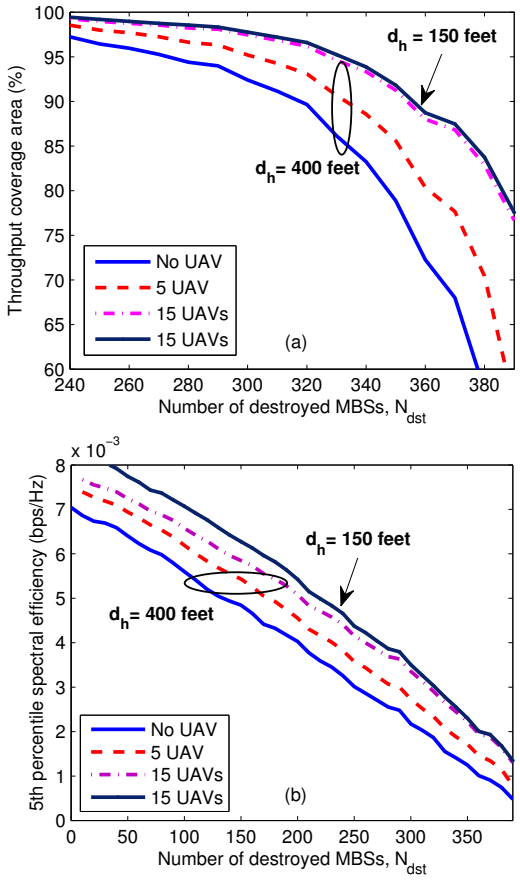

Fig. 6. Improving throughput coverage and 5th percentile SE with UABSs; (a) throughput coverage area versus N_{dst}; (b) 5th percentile SE versus N_{dst}.

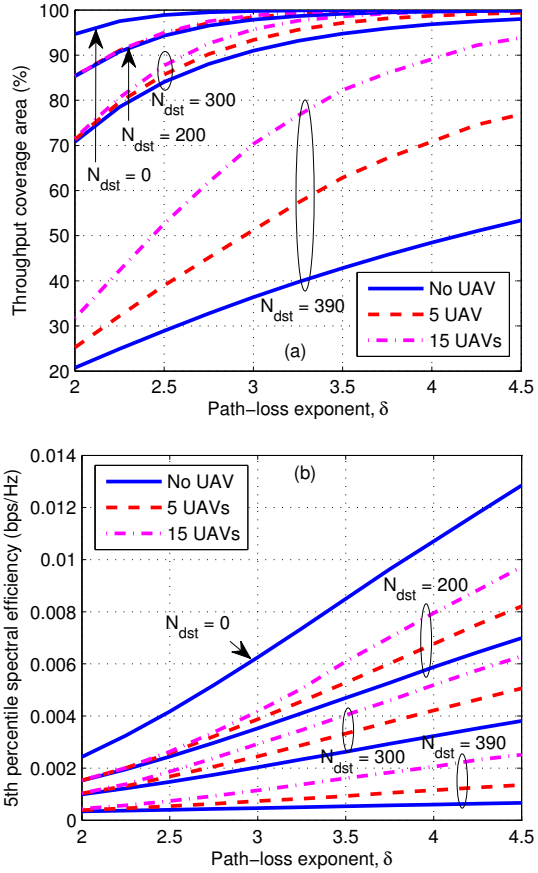

Fig. 7. Effects of PLE on (a) throughput coverage area, and (b) 5th percentile SE.

UABS at every vertex, and the vertex location that maximizes the 5th percentile SE was chosen as the optimum location for UABS.

The throughput coverage area and the 5th percentile SE as a function of the number of destroyed MBSs N_{dst}, (out of a total 400) are shown in Fig. 6, with different number of *helper* UABSs. The throughput coverage area is defined as the percentage of area with throughput larger than a threshold T_{C} (taken as 2.55×10^{-3} bps/Hz in simulations), versus the whole simulation area. These results show that the height (d_{h}) of a UABS has relatively limited effect on throughput coverage, but has a more pronounced effect on the 5th percentile throughput due to path loss factors. Fig. 6 also shows that 15 *optimally-positioned* UABSs can handle the load of up to 70 MBSs from a throughput coverage area perspective, while the gains are lower when the 5th percentile SE is considered. Lowering the UABS height (assuming line-of-sight scenarios) is also shown to bring additional SE benefits due to lower path loss.

The characteristics of throughput coverage and 5th percentile SE with respect to variations in the PLE are shown in Fig. 7. In general, both the throughput coverage and the 5th percentile SE improve with the increasing PLE because the interference power at a UE decreases more rapidly than the signal power as the PLE increases, thereby improving the SIR at the UE. This is due to the fact that the UE's distance to its connected BS is lesser than all other interfering BSs. Fig. 7 also shows that the throughput coverage improves with more number of UABSs, and the improvement is significant with higher PLE. Particularly, the case when 390 out of 400 MBSs are destroyed, approximately 94% of the area can still be covered with just 15 UABSs, provided the PLE is 4.5.

Fig. 8 shows the variations of throughput coverage area and 5th percentile SE with respect to the REB. It can be observed from the figure that the throughput coverage area degrades with increasing REB. As the REB increases, the UABSs can associate with more number of UEs. With the increasing number of UEs in the cell, the average throughput of each user decreases due to the limited spectrum bandwidth available to share among all the UEs in the cell. This causes the throughput coverage area of UABSs to decrease as the REB increases, and motivates further investigations on the use of interference coordination techniques. On the other hand, the effect of REB on the 5th percentile SE is limited. With a careful observation, it can be noted that the 5th percentile SE is maximized at a specific REB

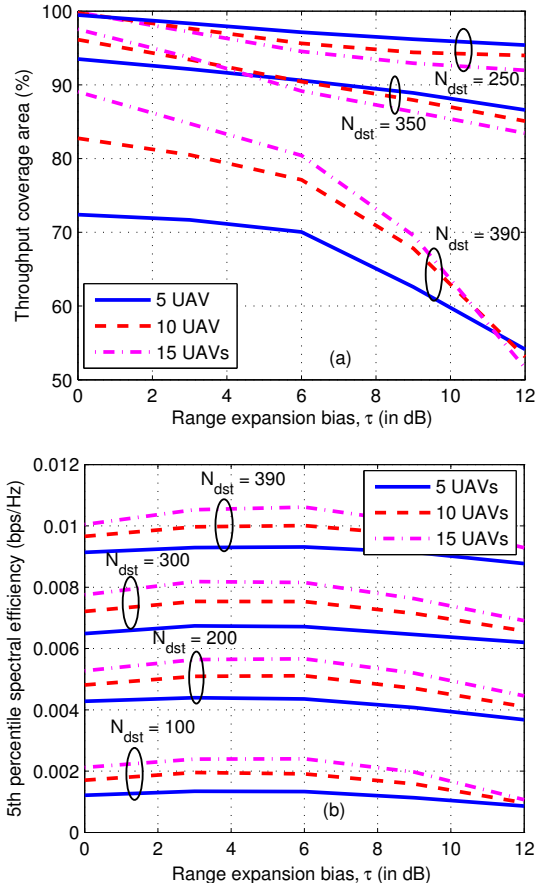

Fig. 8. Effects of REB on (a) throughput coverage area, and (b) 5th percentile SE.

value. However, the difference between the maximum value and the value with $\tau = 0$ dB is not significant.

VI. Concluding Remarks and Discussion

In this paper, we showed that the public safety communications can significantly benefit from deploying UABSs in the event of any damage to the network infrastructure due to natural calamities or malevolent attacks. Through simulations we showed that throughput coverage and 5th percentile capacity of the network can be maximized by optimally placing the UABSs. Higher channel PLE is shown to provide significant improvement in the throughput coverage and 5th percentile capacity of the network. The use of REB for UABSs did not show any significant benefits. However, the potential benefits of REB when used with inter-cell interference coordination techniques is yet to be studied in future. For the purpose of analysis, we used brute force search technique for optimizing the locations of UABSs, although other optimization techniques, including learning algorithms, can be used for optimizing the UABSs' locations. Other directions for future research include studying the impact of UABSs in generalized HetNet scenario (consisting of small-cells such as picocells and femtocells), studying the delay in transmitted messages with non-full buffer traffic model, and developing low-complexity heuristics for UAV placement.

References

[1] G. Baldini, S. Karanasios, D. Allen, and F. Vergari, "Survey of wireless communication technologies for public safety," *IEEE Commun. Surveys Tutorials*, vol. 16, no. 2, pp. 619–641, Second quarter 2014.

[2] United States Government Accountability Office, "Emergency communications: Various challenges likely to slow implementation of a public safety broadband network," Report to Congressional Requesters, Feb. 2012. [Online]. Available: http://www.gao.gov/assets/590/588795.pdf

[3] FCC, "National broadband plan – ch. 16: Public safety," Mar. 2010. [Online]. Available: http://www.broadband.gov/plan/16-public-safety/

[4] J. Andrews, S. Buzzi, W. Choi, S. Hanly, A. Lozano, A. Soong, and J. Zhang, "What will 5G be?" *IEEE J. Select. Areas Commun. (JSAC)*, vol. 32, no. 6, pp. 1065–1082, June 2014.

[5] C. Essid, "Nationwide public safety broadband network," Dept. of Homeland Security, Office of Emergency Communications Report, June 2012. [Online]. Available: http://www.dhs.gov/sites/default/files/publications/Fact%20Sheet_Nationwide%20Public%20Safety%20Broadband%20Network.pdf

[6] International Telecommunications Union, "Radiocommunication objectives and requirements for public protection and disaster relief," ITU-R Report M.2033, 2003. [Online]. Available: http://www.itu.int/dms_pub/itu-r/opb/rep/R-REP-M.2033-2003-PDF-E.pdf

[7] About FirstNet, Website, National Telecommunications and Information Administration, US Dept. of Commerce. [Online]. Available: http://www.ntia.doc.gov/page/about-firstnet

[8] N. B. Johnson, "Are drones and robots the future of public safety?" June 2014. [Online]. Available: http://www.statetechmagazine.com/article/2014/06/are-drones-and-robots-future-public-safety

[9] J. Villasenor, "Drones and the future of domestic aviation," *Proc. of the IEEE*, vol. 102, no. 3, pp. 235–238, Mar. 2014.

[10] C. Barrado, R. Messeguer, J. López, E. Pastor, E. Santamaria, and P. Royo, "Wildfire monitoring using a mixed air-ground mobile network," *IEEE Perv. Computing*, vol. 9, no. 4, pp. 24–32, 2010.

[11] "Amazon Prime Air." [Online]. Available: http://www.amazon.com/b?node=8037720011

[12] L. P. Koh, "A drone's-eye view of conservation," June 2013. [Online]. Available: http://www.ted.com/talks/lian_pin_koh_a_drone_s_eye_view_of_conservation

[13] "Google Loon project." [Online]. Available: http://www.google.com/loon/

[14] A. Abdulsalam, H. Li, and J. Zhang, "Internet for all: Stratospheric solutions by Google Loon and Facebook drone," Technical Report, Mar. 2014.

[15] "Aerial base stations with opportunistic links for unexpected and temporary events." [Online]. Available: http://www.absolute-project.eu/

[16] M. Kobayashi, "Experience of infrastructure damage caused by the great east Japan earthquake and countermeasures against future disasters," *IEEE Commun. Mag.*, vol. 52, no. 3, pp. 23–29, Mar. 2014.

[17] A. Merwaday, S. Mukherjee, and I. Guvenc, "Capacity analysis of LTE-Advanced HetNets with reduced power subframes and range expansion," *EURASIP J. Wireless Commun. Networking*, 2014.

[18] S. Rohde, M. Putzke, and C. Wietfeld, "Ad hoc self-healing of OFDMA networks using UAV-based relays," *Ad Hoc Networks*, vol. 11, no. 7, pp. 1893–1906, 2013.

[19] E. Yanmaz, S. Hayat, J. Scherer, and C. Bettstetter, "Experimental performance analysis of two-hop aerial 802.11 networks," in *Proc. IEEE Wireless Commun. and Net. Conf (WCNC)*, Istanbul, Turkey, 2014.